COMPUTER SIMULATION AND EXPERIMENTAL RESEARCH OF THE VEHICLE IMPACT

DANIEL TRUSCA, ADRIAN SOICA, BOGDAN BENEA, STELIAN TARULESCU
Department of Mechanical Engineering
Transylvania University of Brasov
Eroilor Boulevard, No 29, Brasov
ROMANIA
d.trusca@unitbv.ro

Abstract: - This paper investigates the vehicle rear impact and its consequences and analyzes the research developed in this field. In road traffic, especially in urban traffic, numerous rear collisions have taken place, resulting in serious injuries for passengers. The numerous studies that have been carried out lead to today's internationally recognized demand on the car driver's head restraint adjustment for an optimal protection of the neck spinal column (HWS) with regard to rear end collisions. Mathematical modeling of passenger movement during head impact may be a successful tool in establishing the neck injury mechanism, especially when working in parallel with experimental studies. In order to accomplish experimental studies for data acquisition and video and image samples analysis, the preparation of testing device are needed. Validation mathematical models using experimental tests, offers a vast range of their use. Thus, the simulation on the computer of the phenomena that take place during road events can be studied more comprehensively, and may allow optimize passive safety systems in order to diminish adverse effects of these phenomena.
Key-Words: - modeling, collision, simulation, experimentation, safety, validation

1 Introduction

Vehicle safety is a phenomenon that more and more specialists who are directly involved in the industry vehicles or in a field complementary. The explanation lies in their desire to improve the current concept of possible safety car, but also to distinguish the design of equipment and systems performances. By forging mathematics of road events is obtained important data to help improve safety liabilities of motor vehicles. By using mathematical models, human bodies are most often imprinted extensive movements. They are according to the complexity of simple mono-body models, the type mass- elastic element until three-dimensional models of the whole body. Generally, they assimilate man with a crisp element linked by different types of joints, into a system with open loop.

2 Modeling rear collision between two vehicles

Modeling rear impact by a model of vibration theory involves the use of a mathematical model that simply consists of two masses linked with a spring for global rigidity C. The contact spring represents global rigidity two vehicles entering the collision front/rear. This model is used to theoretically determine functions of the time of speed, acceleration and deformation of the motor vehicles in front/rear centered impact.

2.1 Determining theoretical functions of the time of speed, acceleration and deformations of the motor vehicles in centered rear impact

The simplified mathematical model consists of two masses linked with a spring for global rigidity C. [8]

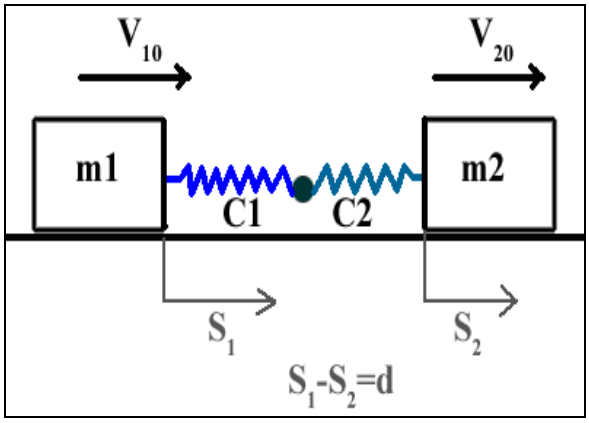

Fig.1 The scheme of crash model between two vehicles assimilated of a theory vibrations model

Noting with, index 1 the vehicle moving from behind and with 2 at the front, resulting global rigidity:

$$\frac{1}{C}=\frac{1}{C_1}+\frac{1}{C_2}; \tag{1}$$

Considering vehicles coming into collision that two masses coupled with one another in a spring of rigidity C, equations of movement have the form:

$$m_1\cdot\frac{d^2s_1}{dt^2}=-C\cdot(s_1-s_2); \tag{2}$$

$$m_2\cdot\frac{d^2s_2}{dt^2}=C\cdot(s_1-s_2); \tag{3}$$

From the first relation is obtaining:

$$\frac{m_1}{C}\cdot\ddot{s}_1+s_1=s_2, \tag{4}$$

After a second derivation replace in relation (3), there results an IV order differential homogeneous equation:

$$\frac{m_1\cdot m_2}{C}\cdot s_1^{(IV)}+(m_1+m_2)\cdot s_1^{(II)}=0; \tag{5}$$

The characteristic equation is:

$$\frac{m_1\cdot m_2}{C}\cdot\lambda^4+(m_1+m_2)\cdot\lambda^2=0; \tag{6}$$

Where:

$$\lambda_1=0;$$
$$\lambda_2=0; \tag{7}$$

$$\frac{m_1\cdot m_2}{C}\cdot\lambda^2+(m_1+m_2)=0; \tag{8}$$

$$\lambda_{3/4}=\pm j\cdot\sqrt{\frac{(m_1+m_2)\cdot C}{m_1\cdot m_2}}\ =\ \pm j\omega; \tag{9}$$

ω – system rhitmic variation

For the first vehicle:

General solution for calculation of the space (covered distance in deformation) it is formed by next equation:

$$s_1=A\cdot t+B\cdot t^2+R\cdot\sin\omega t+D\cdot\cos\omega t \tag{10}$$

The velocity of vehicle 1 depending on time:

$$v_1=\dot{s}_1=A+2\cdot B\cdot t+\omega\cdot R\cdot\cos\omega t-\omega\cdot D\cdot\sin\omega t; \tag{12}$$

Negative acceleration :

$$a_1=\ddot{s}_1=2\cdot B-\omega^2\cdot R\cdot\sin\omega t-\omega^2\cdot D\cdot\cos\omega t\ ; \tag{13}$$

In similar way, for the second vehicle:

$$s_2=\frac{m1}{C}\cdot(2\cdot B-\omega^2\cdot R\cdot\sin\omega t-\omega^2\cdot D\cdot\cos\omega t)+$$
$$+A\cdot t+B\cdot t^2+R\cdot\sin\omega t+D\cdot\cos\omega t; \tag{14}$$

$$v_2=\dot{s}_2=\frac{m_1}{C}\cdot(-\omega^3\cdot R\cdot\cos\omega t+\omega^3\cdot D\cdot\sin\omega t)+$$
$$+A+2\cdot B\cdot t+\omega\cdot R\cdot\cos\omega t-\omega\cdot D\cdot\sin\omega t \tag{15}$$

$$a_2=\ddot{s}_2=\frac{m_1}{C}\cdot(\omega^4\cdot R\cdot\sin\omega t+\omega^4\cdot D\cdot\cos\omega t)+$$
$$+2\cdot B-\omega^2\cdot R\cdot\sin\omega t-\omega^2\cdot D\cdot\cos\omega t \tag{16}$$

Integration constants results from the initial coditions:

$$\begin{cases}A=v_{10}+(v_{10}-v_{20})\cdot\dfrac{C}{\omega^2\cdot m_1};\\ B=0;\\ D=0;\\ R=(v_{10}-v_{20})\dfrac{C}{\omega^3\cdot m_1};\end{cases} \tag{17}$$

This relation is invalid at the end of copresion phase, when:

$$\omega\cdot t=\frac{\pi}{2} \tag{18}$$

and

$$\omega=\frac{\pi}{2\cdot t} \tag{19}$$

Replacing integration constants, there is obtained:

For vehicle 1

$$s_1=\left[v_{10}+(v_{10}-v_{20})\cdot\frac{C}{\omega^2\cdot m_1}\right]\cdot t+(v_{10}-v_{20})\frac{C}{\omega^3\cdot m_1}\cdot\sin\omega t \tag{20}$$

$$v_1=\dot{s}_1=v_{10}+(v_{10}-v_{20})\cdot\frac{C}{\omega^2\cdot m_1}+\omega\cdot(v_{10}-v_{20})\frac{C}{\omega^3\cdot m_1}\cdot\cos\omega t; \tag{21}$$

$$a_1=\ddot{s}1=-\omega^2\cdot(v_{10}-v_{20})\frac{C}{\omega^3\cdot m_1}\cdot\sin\omega t;$$

(22)

For vehicle 2

$$s_2 = \frac{m1}{C}\cdot\left(-\omega^2\cdot(v_{10}-v_{20})\frac{C}{\omega^3\cdot m_1}\cdot\sin\omega t\right)+$$
$$+(v_{10}-v_{20})\frac{C}{\omega^3\cdot m_1}\cdot\sin\omega t+$$
$$+v_{10}+(v_{10}-v_{20})\cdot\frac{C}{\omega^2\cdot m_1}\cdot t;$$

(23)

$$v_2=\dot{s}_2=\frac{m1}{C}\cdot\left(-\omega^3\cdot(v_{10}-v_{20})\frac{C}{\omega^3\cdot m_1}\cdot\cos\omega t\right)+v_{10}+$$
$$+(v_{10}-v_{20})\cdot\frac{C}{\omega^2\cdot m_1}+\omega\cdot(v_{10}-v_{20})\frac{C}{\omega^3\cdot m_1}\cdot\cos\omega t$$

(24)

$$a_2=\dot{s}_2=\frac{m_1}{C}\cdot\left(\omega^4\cdot(v_{10}-v_{20})\frac{C}{\omega^3\cdot m_1}\cdot\sin\omega t\right)$$
$$-\omega^2\cdot(v_{10}-v_{20})\frac{C}{\omega^3\cdot m_1}\cdot\sin\omega t;$$

(25)

The results of the equations of movement for the two vehicles are as follows:

For vehicle 1:

$$\begin{cases} s_1=\left[v_{10}+(v_{20}-v_{10})\cdot\frac{C}{m_1\cdot\omega^2}\right]\cdot t-(v_{20}-v_{10})\cdot\frac{C}{m_1\cdot\omega^3}\cdot\sin\omega t; \\ v_1=\dot{s}_1=v_{10}+(v_{20}-v_{10})\cdot\frac{C}{m_1\cdot\omega^2}\cdot(1-\cos\omega t); \\ a_2=\ddot{s}_1=(v_{20}-v_{10})\cdot\frac{C}{m_1\cdot\omega}\cdot\sin\omega t. \end{cases} \quad (26)$$

For vehicle 2:

$$\begin{cases} s_2=\frac{(v_{20}-v_{10})}{\omega}\cdot\sin\omega t\cdot\left(1-\frac{C}{m_1\cdot\omega^2}\right)+\left[v_{10}+(v_{20}-v_{10})\cdot\frac{C}{m_1\cdot\omega^2}\right]\cdot t; \\ v_2=\dot{s}_2=(v_{20}-v_{10})\cdot\cos\omega t+v_{10}+(v_{20}-v_{10})\cdot\frac{C}{m_1\cdot\omega^2}\cdot(1-\cos\omega t); \\ a_2=\ddot{s}_2=(v_{20}-v_{10})\left(\frac{C}{m_1\cdot\omega}-\omega\right)\cdot\sin\omega t. \end{cases} \quad (27)$$

Maximum amplitude are to be determined by the time compression t_c when:

$$\omega\cdot t_c=\frac{\pi}{2}; \quad (28)$$

$$\sin\omega t=1; \quad (29)$$

Introducing in equations, resulting:

For vehicle 1:

$$s_1=\left[v_{10}-v_{10}\cdot\frac{C}{m_1\cdot\omega^2}\right]\cdot t+v_{10}\cdot\frac{C}{m_1\cdot\omega^3}$$
$$\dot{s}_1=v_{10}-v_{10}\cdot\frac{C}{m_1\cdot\omega^2}\cdot \quad ; \quad (30)$$
$$\ddot{s}_1=-v_{10}\cdot\frac{C}{m_1\cdot\omega}$$

For vehicle 2:

$$s_2=-\frac{v_{10}}{\omega}\cdot\left(1-\frac{C}{m_1\cdot\omega^2}\right)+\left[v_{10}-v_{10}\cdot\frac{C}{m_1\cdot\omega^2}\right]\cdot t$$
$$\dot{s}_2=v_{10}-v_{10}\cdot\frac{C}{m_1\cdot\omega^2} \quad ; \quad (31)$$
$$\ddot{s}_2=-v_{10}\cdot\left(\frac{C}{m_1\cdot\omega}-\omega\right)$$

From the relationship with pulsation (rhythmic variation) during compression caused result global rigidity C:

$$\omega=\frac{\pi}{2\cdot t_c}; \qquad \omega=\sqrt{\frac{(m_1+m_2)\cdot C}{m_1\cdot m_2}}; \quad (32)$$

$$\Rightarrow \quad C=\frac{\omega^2\cdot m_1\cdot m_2}{m_1+m_2}; \quad (33)$$

$$\Rightarrow \quad C_{1,2}=C\cdot\frac{d}{d_{1,2}}; \quad (34)$$

Since :

$$C=\frac{C_1\cdot C_2}{C_1+C_2}; \quad (35)$$

=>

$$C_1=C\cdot\frac{d}{d_1} \quad (36)$$

and

$$C_2=C\cdot\frac{d}{d_2} \quad (37)$$

From definition of the deformation equivalent energy there is obtained:

$$C\cdot(d_{din}\cdot d_{st})=EES^2\cdot m_{tot}; \quad (38)$$

Where

$$d_{din}=1.1\cdot d_{st}; \quad (39)$$

And

$$m_{tot} = m_1 + m_2; \quad (40)$$

$$\Rightarrow C \cdot d_{st}{}^2 \cdot 1.1 = EES^2 \cdot m_{tot}$$

$$EES = d_{st} \cdot \sqrt{\frac{1.1 \cdot C}{m_{tot}}} \quad (41)$$

and

$$EES = \frac{d}{1.1} \cdot \sqrt{\frac{1.1 \cdot C}{m_{tot}}} \quad (42)$$

Since:

$$\frac{m_1 \cdot EES_1^2}{2} + \frac{m_2 \cdot EES_2^2}{2} = \frac{(m_1 + m_2) \cdot EES^2}{2}; \quad (43)$$

$$\frac{m_1 \cdot EES_1^2}{2} + \frac{m_2 \cdot EES_2^2}{2} = \frac{C \cdot d_{st}{}^2 \cdot 1.1}{2}; \quad (44)$$

$$\frac{1}{2} \cdot m_1 \cdot EES_1^2 = \frac{1}{2} \cdot C_1 \cdot d_{st1} \cdot d_1; \quad (45)$$

$$\frac{1}{2} \cdot m_2 \cdot EES_2^2 = \frac{1}{2} \cdot C_2 \cdot d_{st2} \cdot d_2;$$

$$d_1 = d_{st1} + 0.1 \cdot d_{st1} = 1.1 \cdot d_{st1}; \quad (46)$$

$$d_2 = 1.1 \cdot d_{st2};$$

d_1 – dynamic deformation is major with 10%, than measured static deformation after the impact collision.

$$\frac{m_1 \cdot EES_1^2}{m_2 \cdot EES_2^2} = \frac{C_1}{C_2} \cdot \frac{d_1}{d_2}; \quad (47)$$

and $$EES = d_{st} \cdot \sqrt{\frac{1.1 \cdot C}{m_{tot}}}; \quad (48)$$

$$d_1 = d_{st1} + 0.1 \cdot d_{st1} = 1.1 \cdot d_{st1}; \quad (49)$$

$$d_2 = 1.1 \cdot d_{st2}; \quad (50)$$

Where:

$s_{1,2}$ – distance covered by the vehicle 1 and 2, during the phase of compression;

C – The coefficient of global rigidity, $C_{1,2}$ – Vehicle rigidity coefficient 1 and 2

d – Global deformation, $d_{1,2}$ – deformation (d_{st} + d_{din}) during compression time of vehicle 1 and 2; d_{st} – static deformation; d_{din} –dynamic deformation;

d – Dynamic deformation is higher than the approximately 10 percent static deformation measured after impact.

EES- Equivalent Energy of Deformation Speed.

2.2 Front-rear collision modeling between two vehicles using dedicated software

The simulation of two motor vehicles impact used the PC-Crash application. [5] In order to determine acceleration variations of vehicle occupant head and torso, in correlation with pusher vehicle speed, the researchers simulated the collision between two vehicles; the speed of the pusher vehicle ranged from 15km/h to 70 km/h and a human model was located in driver's seat in the pushed vehicle.

Fig. 2 Images of vehicle pushed, obtained from the PC-Crash and simulation video during the experiment

In the simulation program there have been inserted two vehicles corresponding models of cars used in experimental phase.

Vehicles are chosen from the database being inserted into the window with a rudimentary spatial form which respects characteristics geometry of real vehicles but did not have a form of bodywork fine detail. To achieve simulations of collision at the rear end to meet as in detail with reality structures type "masch" may be imported, that is a surface designed in detail the bodywork type of desirable vehicle. To properly position the motor vehicles before impact and to identify their final positions, a sketch of test polygon is introduced in space work.

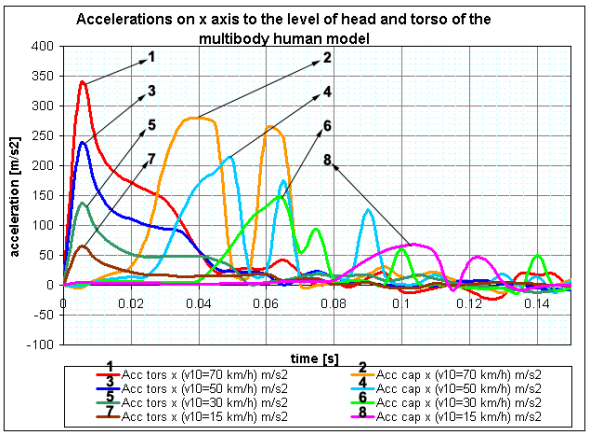

Fig.3 The curve of the acceleration on x axis determined for multi-body system term varying speed v_{10} of pusher vehicle [8]

Modeling rear impact between two motor vehicles, shows that during the appearance of peak of the head acceleration, varies at t_1= 0.035 s for v_{10}= 70 km/h of pusher vehicle, up to t_2=0.105 s for v_{10}= 15 km/h of pusher vehicle.

3 NUMERICAL SOLUTIONS FOR MATHEMATICAL MODEL OF REAR COLLISION

For the numerical solving of the mathematical model there have been introduced values masses vehicles used in the experimental, the speeds of impact and the compression times determined by the experiment.

In order to define the experimental tests the following situations were considered as representative for the impact of two vehicles [7]:

- A vehicle is stationary, no speed recorded V_{20}=0;
- Test1: Pusher vehicle speed V_{10}=18.46 km/h;
- Test2: Pusher vehicle speed V_{10}=26.4 km/h.

The vehicles speed has resulted by integration of the acceleration measured on x axis with Datalogger device. Knowing the fall in the pusher vehicle speed and its growth for the pushed vehicle, they can find compression time per these overlapping curves. Knowing the decrease of the pusher vehicle speed and its growth for the pushed vehicle, they can find compression time by these overlapping curves.[8]

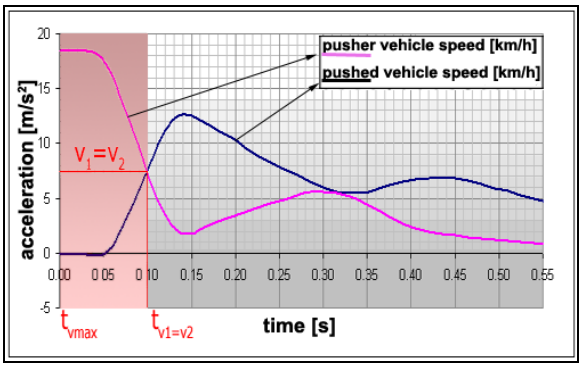

Fig. 4 Determining compression time for v_{10}=18, 46 km/h => t_c=-0.37+0.10=0.063s

By analyzing decreasing and increasing speeds of those two motor vehicles, the compression time can be determined, within the time intervals ranging between t_{vmax} and t_{v1}=t_{v2}.

Where t_{vmax} is the time when v_{10} begin to decrease, and $t_{v1=v2}$ is time when the speeds of those two vehicles are equal.

The time t_c=0.045…0.075s is obtained from diagrams measurements:

$$v_{10} = 14...70 km/h;$$
$$v_{20} = 0 km/h;$$
$$m_{1(mveh1+moccupant)} = 948 kg;$$
$$m_{2(mveh2+moccupant)} = 1253 kg;$$
$$He\ asks: d_{st1} = ?\, d_{st2} = ?$$

Using the compression time there has been determined pulse system of bodies connected by springs treated stiffness like, and thus the coefficient of stiffness is depending on the compression time and determining static alteration resulting on two vehicles involved in conflict.

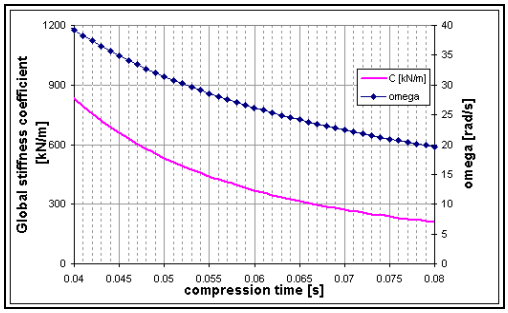

Fig. 5 The variation of the global rigidity coefficient C and the pulsation Omega depending on the compression time tc

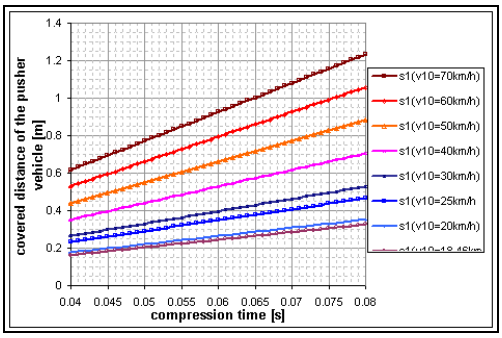

Fig. 6 The change in covered space s1, by pusher vehicle depending on the compression time tc

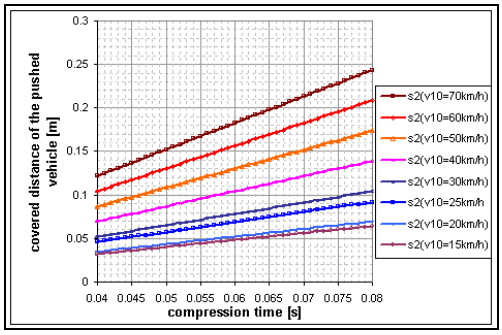

Fig. 7 The change in covered space s2, by pushed vehicle depending on the compression time tc

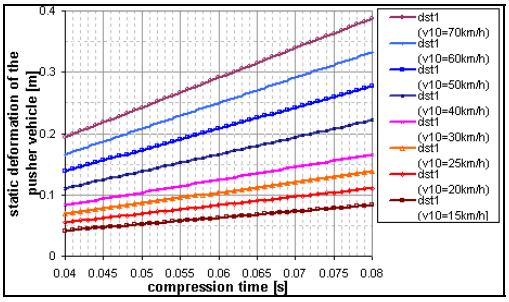

Fig. 8 The change in the static deformation pusher vehicle depending on the stiffness coefficient

Space covered by vehicle and overall deformation during compression depends on the rigidity coefficient, and the compression time.

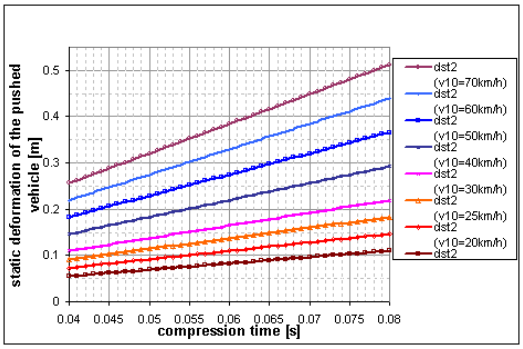

Fig. 9 The change in the static deformation of the pushed vehicle depending on the stiffness coefficient

During the compression phase when the speeds of the two vehicles are equal, motor vehicles deformations are elastic, so that dynamic deformations differs with about 10 percent from the static ones measured after the compression phase..[8]

4 Tests preparation for sampling video

4.1 Preparation of the pushed vehicle

In case of an experiment involving the impact of two vehicles, after polygon area test preparation and ensuring brightness needed by speed video camera, the test vehicles prepared by various areas of the delineation impact paint by marking the squares.

- The areas were marked with linear squares and rims, after the system adopted by EuroNCAP in order to facilitate the analysis of the image of the film.
- The right front door of the car was dismantled in order to ensure the visibility to dummy movements in interval of impact.

Fig. 10 Dismantling right front door to provide visual space for the dummy during rear collision

Fig.11 Painting on areas of the impact of the surfaces bodies vehicles

Fig. 12 Pictures with both painted vehicles

Fig. 13 Rim marcking

Fig. 14 Marking areas car

In order to provide sufficient data for interpretation of car movement, linear squares were marked on the body car surfaces.

4.2 Marking interior of the car

Inside the car pushed it has effectuated sticking the guiding targets for measurement. This was done in accordance with figure 3, for taking measurements post test through video analysis test.

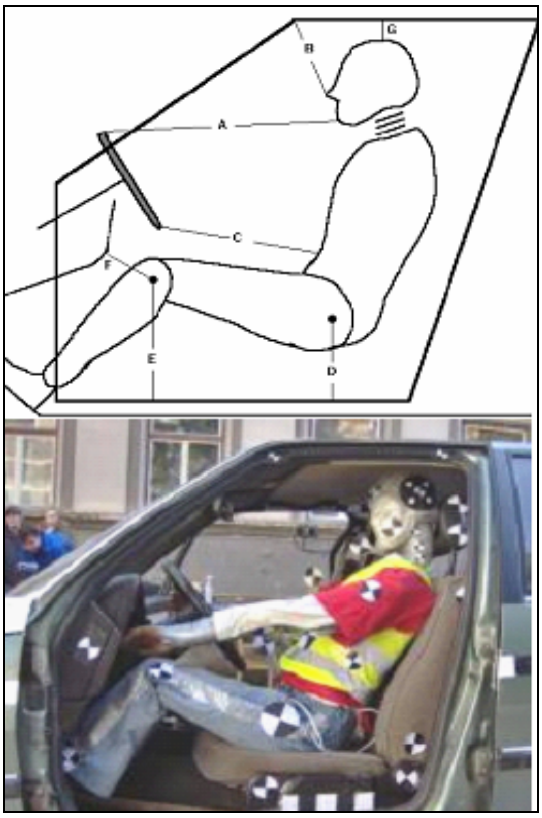

Fig. 14 Marking interior of the car

Table 1. Measurements relating to dummy

A1	chin to the steering wheel
B2	at nose on the top of the windscreen
C3	at torso on steering wheel
D4	H-point threshold on the edge
E5	At the edge-knee threshold
F6	knee at the edge of the column of direction
G7	head to the roof surface
θ8	Neck angle
α9	Back rest angle

4.3 Positioning targets the dummy

Positioning targets on the chair

- For the secvential video's analysis, the following targets are applied on chair.
- T2 – On the head restraint, the high point CG the Head
- T3 – on the back reast at the same height and-neck
- T4 – on the back reast at the same like in fig.4 relative to H point

Point's location (targets) B1, B2 and P is optional. Points T11 and T12 are located on the head dummy, TT1 is the point used to determine speed T1.

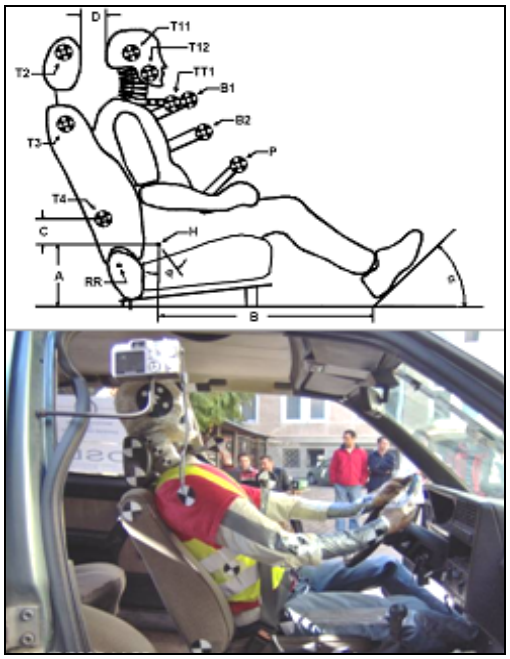

Fig. 15 Marking the car ocupant dummy under ECE-R 94 şi ECE-R 25.

5 Video data-processing

5.1 Squares method

The squares method is used to determine the space covered by the pushed vehicle and its deformation. For the video analysis of samples, the number of squares from left and right side of the pushed vehicle measurement squares line of was required.

For correlation data between numbers of squares on each side of the vehicle, the squares have been counting on both sides of vehicle, separately on each side component of car body.

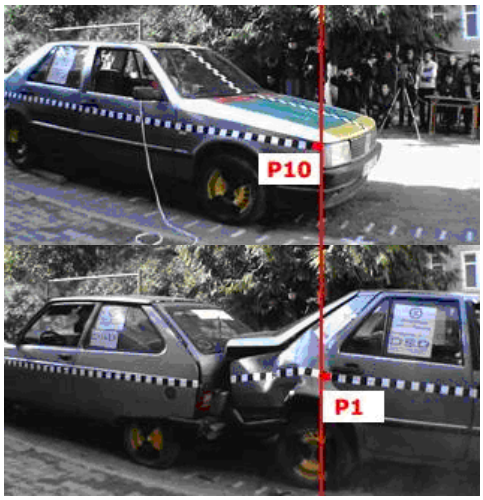

Fig. 16 Determining the covered distance by on the right side of the phused vehicle in video probe for v10= 26.4 km/h

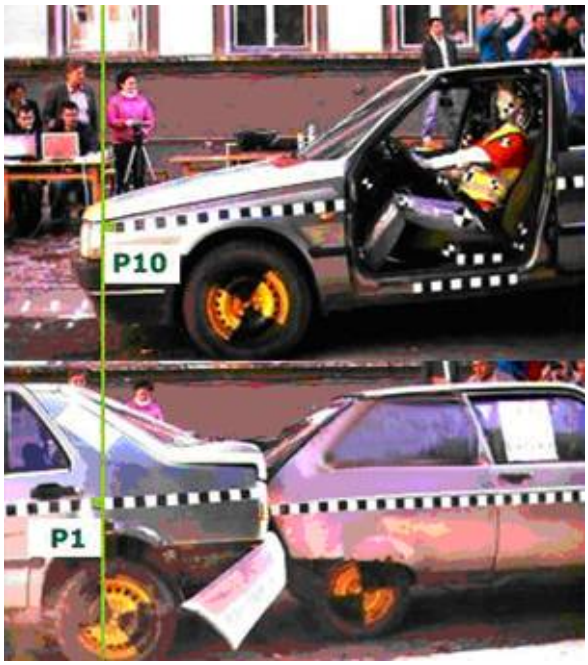

Fig. 17 Determining the covered distance by on the left side of the phused vehicle in video probe for v10= 26.4 km/h

In order to determine the distance covered by the pushed vehicle, on the video recording a line of reference was considered, which took into account the squares succession the bodywork vehicle.

$s_2 = (P_{mudguard} + P_{fronf\ door} + P_{back\ door} + a) \cdot LP$

$d_{2st}=(Ln-Ld)$

Where:

d_{2st}- total static surfaces of the pushed vehicle

a- the number of squares elected on the opposite side of the line of reference

Fig. 18 Deformation measurement, the frame analysis

5.2 Displacement of dummy determination during impact using video analysis of sample

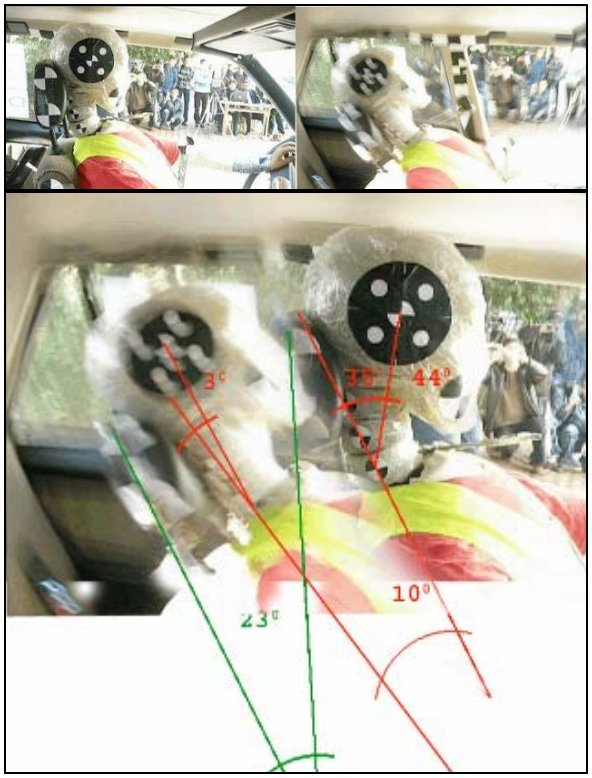

Fig.19 Determining maximum angle of your head, torso and head restraint by film analysis room fitted inside the car

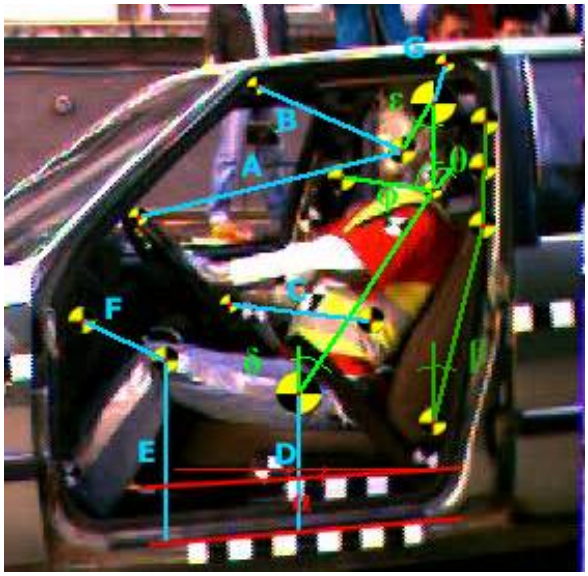

Fig.20 Determining the distances between mounted targets on dummy (before impact).

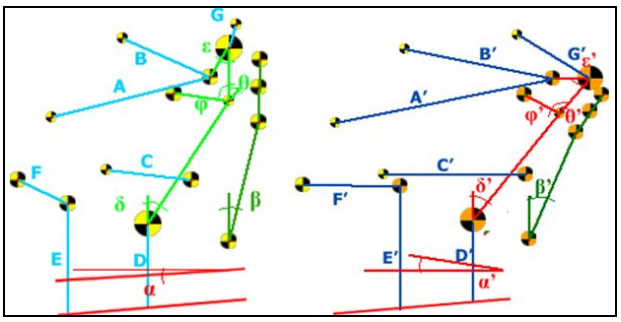

Fig.21 Determining the distances between mounted targets in initial position and maxim backward dummy movements

Table 2. Determined distances between targets

Dimension Measurements betwen targets		Initial position	Maximal backward position	Delta	U.M.
A1	chin to the steering wheel	0.548	0.774	0.226	m
B2	target cheek to the upper part of the windscreen	0.312	0.524	0.212	m
C3	Lower at torso on steering wheel	0.283	0.495	0.212	m
D4	H-point threshold on the edge	0.269	0.277	0.007	m
E5	At the edge-knee threshold	0.354	0.422	0.067	m
F6	knee at the edge of the column of direction	0.180	0.340	0.161	m
G7	head to the roof surface	0.080	0.295	0.215	m
H	Moving horizontally to point H			0.108	
alfa	Backrest angle	4	11	7	grade
beta	The bench seat	14	24	10	grade
delta	The angle between vertical line H line and T1 target	34	40	6	grade
epsilon	The angle between chin-head CG line and T1 axa	30	51	21	grade
fi	The angle between exterior target T1 and line T1-head CG	83	101	18	grade
teta	Neck angle	34	3	31	grade

6 Conclusion

By comparing the experimentally and mathematically obtained data the researchers were able to determine:

- Uncertainty between the parameters determined by simulation using specialized applications and the values experimentally measured.
- Uncertainty between the model of vibration theory and experiment.

The researchers compared the variations of the dummy's torso and head acceleration (in the experimentally test), as well as the accelerations of the multi-body in the simulation conducted by PC-Crash. Consequently, there have been compared the theoretically determined values of deformation at the end of compression, i.e. the dynamic deformation, and the experimentally determined values, i.e. remanent deformation; the first two tests considered a difference of 10 percent between the dynamic and static deformation.

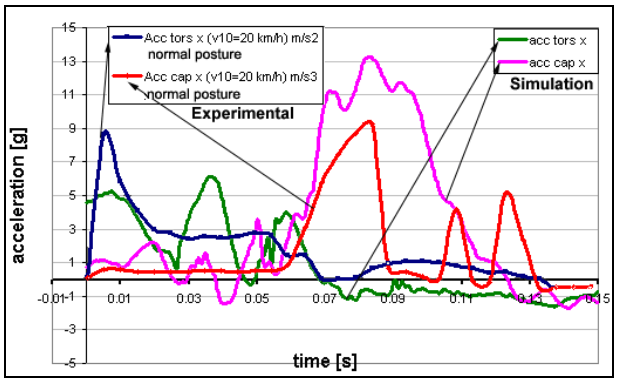

Fig. 21 The curve of the acceleration on x axis in simulation and experimental determinations for v_{10} = 19.44 km/h of pusher vehicle

A comparison between the two diagrams shows an accurate calculation of the parameters that stress the dummy's components. In terms of quality a distinction between experiment and simulation is also noticed. This distinction is particularly caused by the seat rigidity. The simulation could not consider all the characteristics of rigidity of the seat. The experiment shows an oscillation of torso acceleration in the first 50 ms in time.

During the simulation this variation is partly damped. For a speed of the pusher vehicle of 20 km/h, the maximum head acceleration is 10 g on simulation and 13 g on the experiment, the difference is explained by rigidity links between bodies, the multi-body system of the occupant.

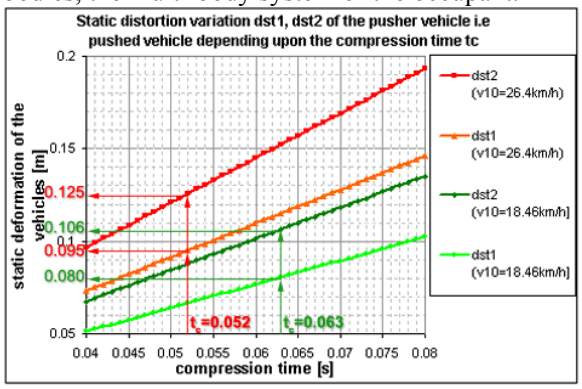

Fig. 22 The determination of vehicles static deformations from the theoretical model diagram of vibration theory

Therefore, for the compression time t_c = 0.063 s and a speed of the pusher vehicle of 18.47 km/h there was determined a calculated value of the static deformation of 0.106 m, and after the first test there has been measured a deformation of the pusher vehicle driven by 0.10 m. For the pusher vehicle, the deformation measured after the first test was 0.08 m, which corresponds to the value calculated by the mathematical formula (see Table 1.).

Table 3. Comparing the theoretical and experimental results

Speed/ Compression time	Theoretical determination d [m]; v[km/h]	Experimental determination d [m]; v[km/h]
v_{10}=18.46km/h tc=0.063 s	d_{1st}= 0.080	d_{1st}= 0.080
	d_{2st}= 0.1064	d_{2st}= 0.100
	v_1=v_2=7.95	v_1=v_2=7.5
v_{10}=26.4km/h tc=0.052 s	d_{1st}= 0.0950	d_{1st}= 0.082
	d_{2st}= 0.1256	d_{2st}= 0.100
	v_1=v_2=11.37	v_1=v_2=12.00

The differences noticed in table 1, between the theoretically and experimentally determined values, during test 2, at a speed $v_{10\ of}$ 26.4 km/h, are due to the fact that the vehicles involved have suffered deformations and throughout the test 1 as well, which led to the modification over the rigidity coefficient. However, the values compared during the test 2 provides the possibility to validate the mathematical model because the differences do not exceed the margin of error by 10%.[8]

References:

[1] Soica A.; Lache S. (2007), - Theoretical and Experimental Approaches to Motor Vehicle - Pedestrian Collision, 3rd WSEAS '07, Tenerife, Canary Islands, Spain, December 14-16, ISSN 1790-2769, pg. 264-270.

[2] Precup C., Naaji A. (2008) - Software simulation for femur fractures in case of frontal car accidents, WSEAS Transactions on Computers 7 Volume 7, Issue 7, July 2008, Pages 1050-1060.

[3] Muñoz-Moreno E., (2005), - Image registration based on automatic detection of anatomical landmarks for bone age assessment, WSEAS Transactions on Computers, no 11, pp. 1596-1603.

[4] Naaji, A. (2008), - Using computer aided techniques in the dynamic modeling of the human upper limb; July 2008 volume 7 WSEAS Transactions on computers ISSN 1109-2750.

[5] Datentechik, S. (2008) – PC-Crash A Simulation Program for Vehicle Accidents - Technical and Operating Manual, Version 8.2 - November 2008, Linz, Austria.

[6] Gaiginschi R., Filip, I. (2002) - Technical expertise of road accidents. - Technical Publishing House of Bucharest..

[7] Seitz, N., (1993) - Aspects of reconstitution road accidents, - Transylvania University of Brasov.

[8] Trusca D.D., (2008) - Research on improving passive safety of the passenger cars in the rear collision – doctorate thesis - Transylvania University of Brasov.